Compatibility of Poly(butadiene-*co*-acrylonitrile) with Poly(L-lactide) and Poly(3-hydroxybutyrate-*co*-3-hydroxyvalerate)

Eun-Soo Park, Hye Kyung Kim, Jae Hun Shim, Hun Sik Kim, Lee Wook Jang, Jin-San Yoon

Department of Polymer Science and Engineering, Inha University, 402-751 Incheon, Korea

Received 23 June 2003; accepted 11 November 2003

ABSTRACT: Poly(L-lactide) (PLLA) and poly(3-hydrobutyrate-*co*-3-hydroxyvalerate) (PHBV) were blended with poly(butadiene-*co*-acrylonitrile) (NBR). Both PLLA/NBR and PHBV/NBR blends exhibited higher tensile properties as the content of acrylonitrile unit (AN) of NBR increased from 22 to 50 *wt* %. However, two separate glass transition temperatures (T_g) appeared in PLLA/NBR blends irrespective of the content of NBR, revealing that PLLA was incompatible with NBR. In contrast, a single T_g, which shifted along with the blend composition, was observed for PHBV/NBR50 blends. Moreover NBR50 suppressed the crystallization of PHBV, indicating that PHBV was compatible with NBR50. Decrease of both elongation modulus and stress at maximum load was less significant and increase of elongation at break was more pronounced in PHBV/NBR50 blends than in PLLA/NBR50 blends. © 2004 Wiley Periodicals, Inc. J Appl Polym Sci 92: 3508–3513, 2004

Key word: blends; biodegradable; crystallization; rubber

INTRODUCTION

Poly(3-hydrobutyrate-*co*-3-hydroxyvalerate) (PHBV) is a biodegradable plastic synthesized by microbial fermentation. Poly(L-lactide) (PLLA) is made from L-lactic acid, which is one of the metabolites in the human body. As both PHBV and PLLA are originated from natural resources, they are quite biocompatible and often used for medical applications such as artificial skin,[1] medical suture,[2–5] fructured bone fixation,[6,7] and drug delivery system[8,9] because of their relatively low toxicity.

Compounding of the bioplastics with other polymers is frequently employed to improve physical properties, to control biodegradability, or to reduce the production cost. Poly(ε-caprolactone),[10–12] polystyrene,[10] starch,[13] poly(styrene-*co*-acrylonitrile),[14] and starch-*graft*-poly(glycidyl methacrylate)[15] are blended with PHBV or PLLA. Poly(butadiene-*co*-acrylonitrile) (NBR) with the acrylonitrile (AN) content in the range of 18–51 wt % was commercialized. As the AN content increased, NBR exhibited increasing density, faster curing rate, higher stiffness, and better processibility.

In this study, PHBV (3-hydroxyvalerate content: 5 wt %) and PLLA were blended with NBR, whose AN content was in the range of 22–50 wt %. Because NBR is a nondegradable clastomer, PHBV/NBR and PLLA/NBR blends are not suitable for medical purposes. However, they can still be used as materials for leisure articles such as golf tees and hunting gun magazines, which are very hard to recollect after use. Very small-sized particles could subsist after ultimate degradation of the matrix of the blends. However, the residual nondegradable elastomer would not cause a significant effect on the environment because it will not provoke any water-clogging phenomena in soil. Single-use receptacles, collecting bags for organic garbages, and fishing nets, whose recycling after discard is cost-intensive, are another important application for the biodestructable plastics.[16–19] Compatibility of the blends was examined. Tensile properties and thermal characteristics of the blends were also explored.

EXPERIMENTAL

Materials

PLLA (M_w = 140,000, polydispersity index (PDI) = 1.91, Shimazu, Japan), PHBV (HV content, 5 wt %, M_w = 370,000, PDI = 2.10 ICI, UK), and NBR (Scientific Polymer Products, grade 053, 556, 531, USA) were used as received. The polymers were dried *in vacuo* at 40°C for 1 week. Other chemicals were used as received without further purification.

Correspondence to: J.-S. Yoon (jsyoon@inha.ac.kr).

Contract grant sponsor: Basic Research Program of the Korea Science and Engineering Foundation; contact grant number: R01-1999-000-00288-0.

Journal of Applied Polymer Science, Vol. 92, 3508–3513 (2004)

TABLE I
Tensile Properties of PLLA/NBR Blends

Sample code	Blend composition (PLLA/NBR wt %)	*E* modulus (MPa)	Stress at maximum load (MPa)	Elongation at break (%)
PLLA	100/0	1297.0 ± 43.0	65.5 ± 3.23	11.4 ± 1.67
PLLA/NBR22	50/50	115.4 ± 18.9	4.32 ± 0.84	43.5 ± 7.28
PLLA/NBR33	50/50	121.4 ± 9.74	6.32 ± 0.46	52.0 ± 17.4
PLLA/NBR43	50/50	193.5 ± 11.2	8.23 ± 0.46	56.7 ± 16.3
PLLA/NBR50	50/50	188.4 ± 13.7	9.27 ± 0.18	150.8 ± 18.6
PLLA/NBR43	99/1	1129.6 ± 24.1	49.0 ± 2.02	6.66 ± 0.34
PLLA/NBR43	97/3	1084.1 ± 84.6	47.7 ± 4.61	6.72 ± 0.51
PLLA/NBR43	95/5	1098.5 ± 60.2	52.2 ± 2.63	7.93 ± 0.55
PLLA/NBR43	90/10	992.0 ± 47.6	42.2 ± 3.27	8.04 ± 0.67
PLLA/NBR43	80/20	745.9 ± 61.8	28.1 ± 2.40	10.8 ± 1.53
PLLA/NBR43	50/50	193.5 ± 11.2	8.23 ± 0.46	56.7 ± 16.3
PLLA/NBR43	0/100	0.752 ± 0.086	2.51 ± 0.38	897.4 ± 137.5
PLLA/NBR50	99/1	1160.0 ± 26.3	47.5 ± 3.31	6.10 ± 0.27
PLLA/NBR50	97/3	1042.7 ± 37.5	45.0 ± 5.87	8.48 ± 2.33
PLLA/NBR50	95/5	1045.8 ± 101.6	44.8 ± 2.05	17.0 ± 4.61
PLLA/NBR50	90/10	973.0 ± 27.7	41.2 ± 1.23	39.1 ± 8.34
PLLA/NBR50	80/20	746.5 ± 47.5	42.3 ± 4.81	42.3 ± 4.81
PLLA/NBR50	70/30	631.9 ± 19.1	27.5 ± 1.43	77.8 ± 35.1
PLLA/NBR50	60/40	533.1 ± 48.0	21.4 ± 1.28	91.6 ± 12.8
PLLA/NBR50	50/50	188.4 ± 13.7	9.27 ± 0.18	150.8 ± 18.6
PLLA/NBR50	0/100	1.20 ± 0.32	2.26 ± 0.78	2040.5 ± 79.0

TABLE II
Thermal Properties of PLLA/NBR Blends

Code	1st scan T_m		2nd scan T_m		
	T_m (°C)	ΔH_f[a] (J/g of PLLA)	T_m (°C)	ΔH_f (J/g of PLLA)	2nd T_g (°C)
PLLA	172.5	39.0	172.9	29.7	61.9
PLLA/NBR50-90/10	173.3	43.2	174.2	43.0	−10.6 60.2
PLLA/NBR50-50/50	171.9	40.2	172.9	44.0	−9.16 60.0
NBR50	—	—	—	—	−10.3

T_m: melting peak temperature (°C).
[a] ΔH_f: heat of fusion (J/g of PLLA).

Instrumentation

The thermal properties of the polymers were determined by DSC (Perkin–Elmer DSC 7, Norwalk, CT). Thermal history of the products was removed by scanning from 30 to 200°C with the heating rate of 20°C/min. After maintaining at 200°C for 1 min and then cooling down the sample at −200°C/min to −100°C, it was reheated at 20°C/min to 200°C and the second-scan DSC thermograms were obtained.

Tan δ of the specimens (50 × 5 × 0.1mm^t) was measured by using Rheovibron (DDV-II-C, Japan) at a fixed frequency of 110 Hz while heating the sample from −100 to 80°C at a heating rate of 20°C/min. Mechanical properties of the samples were determined with a universal test machine (Instron model 4200, Canton, MA) at a cross-head speed of 50 mm/min according to ASTM D638 at 15 ± 1°C in relative humidity (RH) 65 ± 1%. The sample sheet was fractured while immersed in liquid nitrogen and then etched with *o*-xylene to dissolve out the NBR domains.

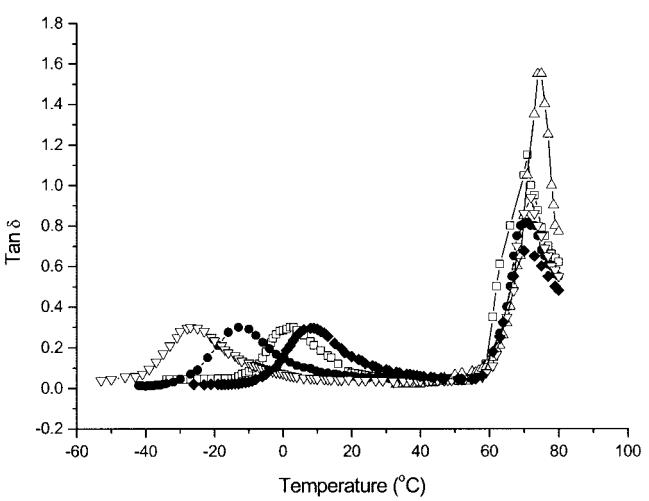

Figure 1 Tan δ curve of PLLA/NBR(50/50) blend system measured at 110 Hz (Δ : PLLA; ▽ : PHBV/NBR22; ● : PLLA/NBR33; □ : PLLA/NBR43; ◆ : PLLA/NBR50).

TABLE III
Tensile Properties of PHBV/NBR Blends

Sample code	Blend composition (PLLA/NBR wt %)	*E.* modulus (MPa)	Stress at maximum load (MPa)	Elongation at break (%)
PHBV	100/0	1118.8 ± 357.6	27.2 ± 8.43	3.94 ± 0.25
PHBV/NBR22	50/50	123.1 ± 11.3	4.07 ± 0.78	38.1 ± 0.89
PHBV/NBR33	50/50	141.9 ± 14.2	5.50 ± 0.89	143.6 ± 1.42
PHBV/NBR43	50/50	134.6 ± 13.8	8.07 ± 1.02	387.8 ± 12.4
PHBV/NBR50	50/50	157.3 ± 15.3	7.95 ± 1.34	405.6 ± 23.5
PHBV/NBR50	99/1	804.9 ± 50.2	25.2 ± 0.86	4.78 ± 0.25
PHBV/NBR50	97/3	761.5 ± 49.1	24.7 ± 2.18	5.35 ± 0.53
PHBV/NBR50	95/5	692.1 ± 37.2	22.7 ± 1.74	5.68 ± 0.89
PHBV/NBR50	90/10	539.2 ± 67.8	21.1 ± 1.85	6.34 ± 1.32
PHBV/NBR50	80/20	530.6 ± 51.7	20.8 ± 0.66	18.0 ± 5.43
PHBV/NBR50	70/30	411.6 ± 34.2	14.5 ± 1.00	70.31 ± 17.53
PHBV/NBR50	60/40	350.4 ± 29.0	11.5 ± 0.44	167.71 ± 13.24
PHBV/NBR50	0/100	1.20 ± 0.32	2.26 ± 0.78	2040.5 ± 79.0

TABLE IV
Thermal Properties of PHBV/NBR50 Blends

Code	1st T_m		2nd T_m		2nd T_g (°C)	2nd T_c	
	Temp. (°C)	ΔH_f (J/g of)	Temp. (°C)			Temp (°C)	ΔH_f (J/g of)
PHBV	160.2	83.8	149.6	161.5	−3.25	46.2	−41.5
PHBV/NBR-99/1	161.0	71.5	149.9	161.7	−3.16	50.1	−43.3
PHBV/NBR-97/3	159.6	69.0	151.9	161.9	−3.29	57.5	−45.2
PHBV/NBR-95/5	160.9	66.2	152.6	162.7	−3.26	59.5	−44.7
PHBV/NBR-90/10	160.2	63.6	152.0	162.1	−3.84	60.4	−40.3
PHBV/NBR-80/20	161.1	68.2	152.9	162.6	−4.15	61.8	−40.9
PHBV/NBR-50/50	160.5	62.7	151.6	162.1	−6.50	54.2	−21.3
NBR50	—	—	—		−10.3	—	—

Scanning electron micrographs (SEM; S-4200, Hitach, Japan) was used to observe the fractured surface morphology. Specimens were made by hot pressing (Lab Press, Carver, OH) at 180°C for 1 min under 3.5 atm followed by convection cooling at room temperature.

Polymer blending

The PLLA/NBR and PHBV/NBR mixtures were dissolved in chloroform. After stirring for 6 h, the blend solution was precipitated in methanol and dried *in vacuo* at 50°C.

RESULTS AND DISCUSSION

PLLA/NBR and PHBV/NBR blends were casted from chloroform solution. After a thorough drying, the sheets of the blends were subjected to thermal analysis on DSC.

Mechanical and thermal properties of PLLA/NBR blends

Table I lists the tensile properties of PLLA/NBR blends. Mechanical properties of the PLLA/NBR50 blend were better than those of the PLLA/NBR22, PLLA/NBR33, and PLLA/NBR43 blends. Table II summarizes thermal properties of the PLLA/NBR50 blends. Melting peak temperature (T_m) and heat of

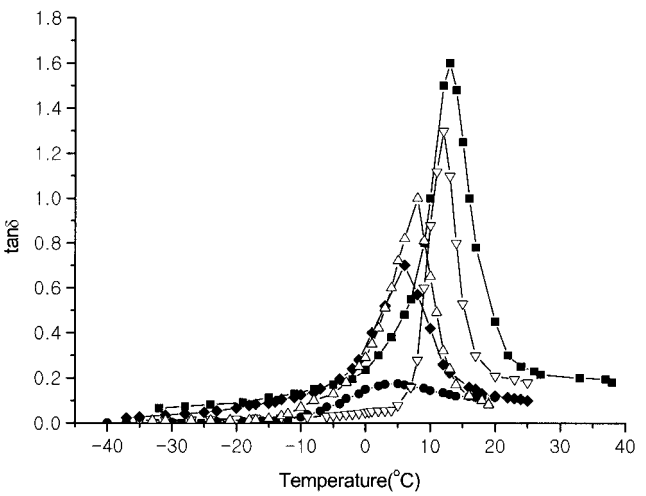

Figure 2 Tan δ curve of PHBV/NBR blend system measured at 110 Hz [■ : PHBV; ▽ : PHBV/NBR50(80/20); △ : PHBV/NBR50(70/30); ◆ : PHBV/NBR50(60/40); ● : PHBV/NBR50(50/50)].

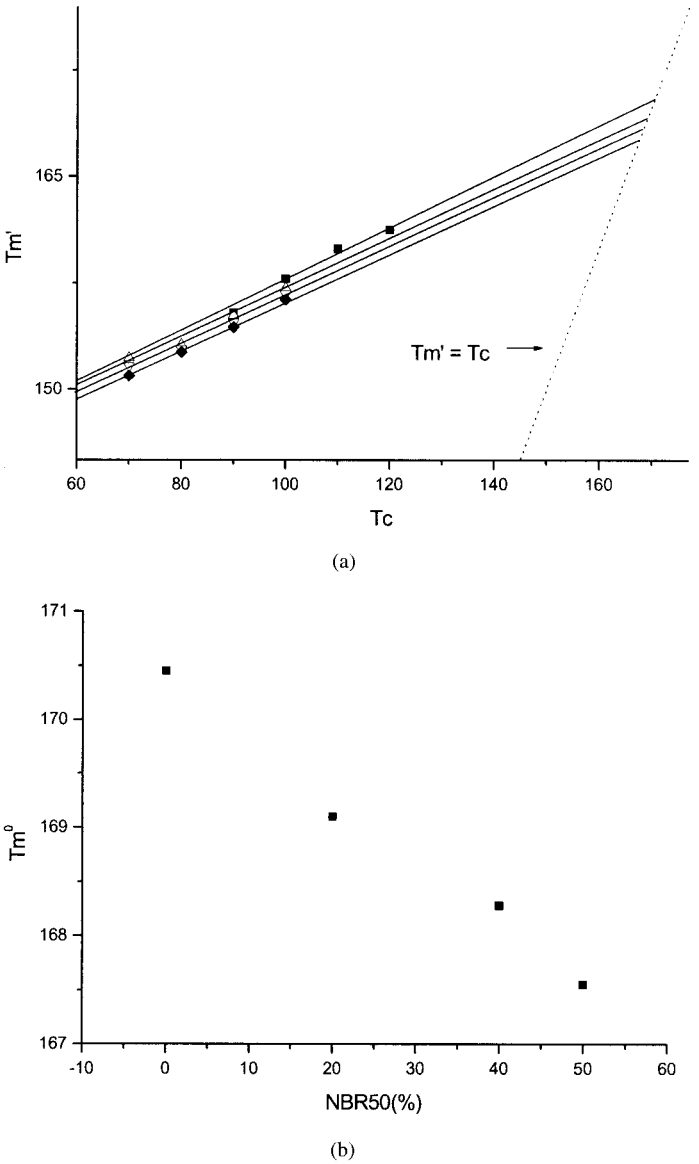

Figure 3 Equilibrium melting temperature of PHBV/NBR50 blends. (a) Representation of melting point temperatures by the Hoffman–Weeks equation [■ : PHBV; △ : PHBV/NBR50(80/20); ▽ : PHBV/NBR50(60/40); ◆ : PHBV/NBR50(50/50)]. (b) Equilibrium melting temperature as a function of the NBR50 content.

fusion (ΔH_f) of PLLA phase remained practically unchanged after blending with NBR50. Moreover, glass transition temperature (T_g) of PLLA/NBR50 blends appeared constant at two fixed temperatures (i.e., at ca. 60 and −10°C, which correspond to T_g of pristine PLLA and that of pristine NBR50, respectively).

Figure 1 shows tan δ profiles of the PLLA/NBR22, PLLA/NBR33, PLLA/NBR43, and PLLA/NBR50 blends. Tan δ peak temperature of NBR increased as the content of AN of NBR increased. Two separate tan δ peaks appeared, and the two tan δ peaks of PLLA/NBR blends located at the same temperatures as those of the corresponding parent polymers. Therefore, it can be concluded clearly that PLLA and NBR are incompatible and phase-separated when the AN content of NBR was in the range of 22–50 wt %.

Mechanical and thermal properties of PHBV/NBR blends

Tensile properties of PHBV/NBR blends are collected in Table III. It can be again perceived that the tensile properties of PHBV/NBR blends became better as the content of AN of NBR increased from 22 to 50 wt %.

Thermal properties of PHBV/NBR50 blends are summarized in Table IV. T_g decreased and crystallization temperature (T_c) increased with the NBR50 content. Figure 2 reveals that only one tan δ peak was observed and moved downward as the NBR50 content increased. Melting temperature (T_m) data of PHBV/NBR50 blends are represented by the Hoffman–Weeks[19] equation. The extrapolation straight lines for the Hoffman–Weeks equation were drawn by using

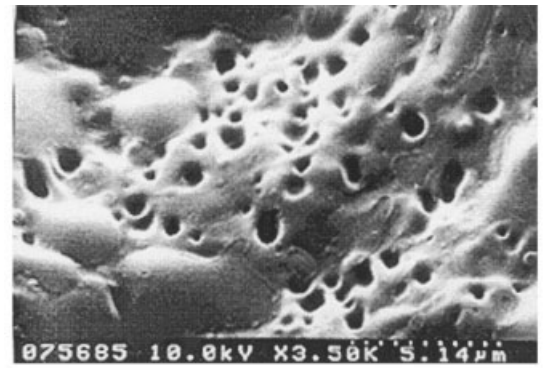

(a)

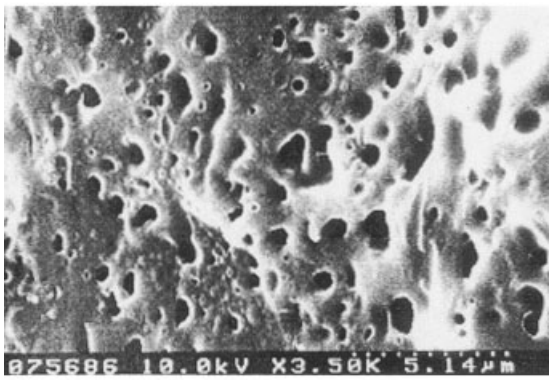

(b)

Figure 4 Scanning electron micrographs (SEM) of PHBV/NBR50 system. (a) PHBV/NBR50 (90/10); (b) PHBV/NBR50 (80/20).

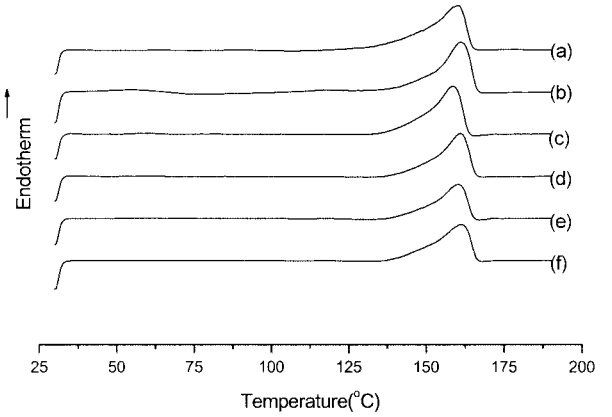

(a)

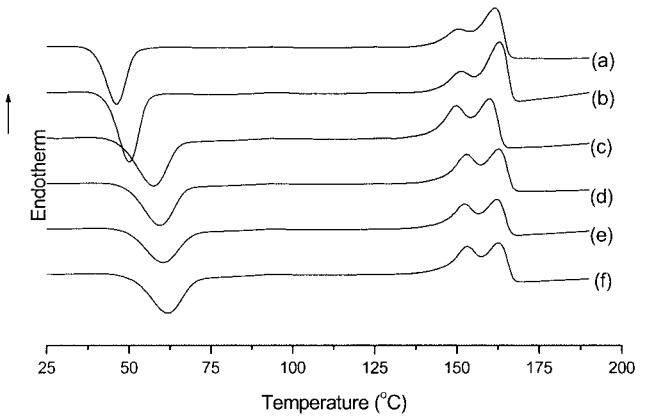

(b)

Figure 5 DSC thermograms of PHBV/NBR50 blends. (a) PHBV; (b) PHBV/NBR50-99/1; (c) PHBV/NBR50-97/3; (d) PHBV/NBR50-95/5; (e) PHBV/NBR50-90/10; (f) PHBV/NBR50-80/20. (a) The first heating scan; (b) The second heating scan.

the least-squares fit. The determined equilibrium melting temperatures (T_m^0) are shown in Figure 3. From the results of T_g, tan δ, T_c, and $T_m°$, it can be concluded obviously that PHBV is compatible with NBR50.

According to Figure 4, NBR50 is not, however, completely miscible in PHBV on a molecular scale. The term compatibility is used here when the blending brings about positive improvement in mechanical properties, even though the constituents are not completely miscible with each other. Enhancement of impact strength of PHBV/NBR50 blends was not as remarkable as was expected (Table V), which should be due in part to the small domain size of NBR50 phase as demonstrated in Figure 4. Elastomer should be neither completely miscible nor completely incompatible with the matrix polymer for the purpose of optimum toughening.[18]

TABLE V
Impact Properties of PHBV/NBR50 Blends

Sample code	Blend composition (PHBV/NBR wt %)	Impact (kg_f cm/cm)
PHBV	100/0	1.69
PHBV/NBR50	99/1	1.96
PHBV/NBR50	95/5	1.93
PHBV/NBR50	80/20	2.51

Crystalization of PHBV/NBR50 blends

Figure 5 demonstrates DSC thermograms of PHBV/NBR50 blends. The specimens for the first-scan DSC thermograms were prepared by hot pressing at 180°C under 3.5 atm followed by natural convection cooling in air. Crystallization of PHBV took place during the slow cooling process, and the PHBV/NBR50 blends exhibited monomodal melting peak in the first-scan DSC thermogram.

The specimens were quenched cryogenically after the first scan and reheated from −100°C at 5°C/min to obtain the second-scan DSC thermograms. Curiously enough, the specimens showed bimodal melting peaks in the second scan DSC thermograms.

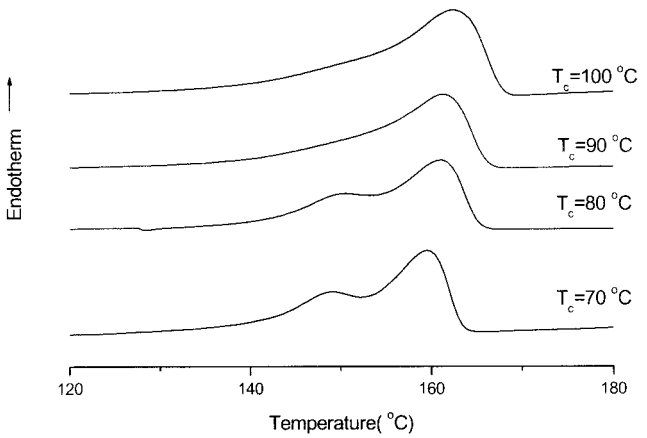

Figure 6 Melting peak profiles of PHBV/NBR50 (99/1 wt %) blend crystallized isothermally for 30 min at 100, 90, 80, and 70°C after quenching from 180°C.

It has been reported that poly(3-hydroxybutyrate) (PHB), on the contrary, demonstrated bimodal melting peak and monomodal melting peak in the first-scan and second-scan DSC thermograms, respectively.[16] Organ and Barham[16] attributed the lower temperature melting peak in the first-scan DSC thermograms of PHB to melting of the as-formed crystals of PHB during the sample preparation, and the high-temperature melting peak to melting of crystals formed by recrystallization during the second-scan heating.

PHBV was quenched by using liquid nitrogen from 180°C to different T_c. Melting peak profiles of PHBV after crystallization at 100, 90, 80, and 70°C for 30 min are shown in Figure 6. PHBV crystallized at higher than 90°C and that crystallized at lower than 80°C for 30 min exhibited unimodal melting peak, and bimodal melting peak, respectively. The higher temperature melting peak of the bimodal peak appeared at a similar temperature as the first-scan melting peak temperature. Less perfect crystals formed at lower crystallization temperature and these crystals were melted and recrystallized during the final heating scan. The higher temperature peak of the bimodal melting peak should due to melting of the recrystallized crystals.

When PHBV was crystallized at a temperature higher than 90°C, the lower melting peak is not discernible and the melting peak is unimodal because those crystals formed are perfect enough that the fraction of the crystals melted and recrystallized during the final heating scan is insignificantly small.

In Figure 5, the crystallization peak during the second scan appeared at a higher temperature as the content of NBR50 in PHBV/NBR50 blends increased, indicating that NBR50 suppressed the crystallization of PHBV.

In the second-scan DSC thermograms of PHBV/NBR50 blends, the lower temperature melting peak increased in intensity compared to the higher temperature melting peak as the content of NBR50 in the blends increased. This can be explained in the same context as above. As the crystallization of PHBV was suppressed with an increase in the NBR50 content, the fraction of crystals recrystallized during the heating scan became smaller so that relative intensity of the higher temperature peak to that of the lower temperature peak decreased.

This work was supported by grant R01-1999-000-00288-0 from the Basic Research Program of the Korea Science and Engineering Foundation.

References

1. Chen, L. J., Wang, M. Biomaterials 2002, 23, 2631.
2. Chun, Y. S., Kim, W. N. Polymer 2000, 41, 2305.
3. Blumm, E., Owen, A. J. Polymer 1995, 36, 4007.
4. Zhang, L., Goh, S. H., Lee, S. Y. Polymer 1998, 39, 4841.
5. Shuai, X., He, Y., Asakawa, N., Inoue, Y. J Appl Polym Sci 2001, 81, 762.
6. Gajria, A. M., Dave, V., Gross, R. A., McCarthy, S. P. Polymer 1996, 37, 437.
7. Eguiburn, J. L., Iruin, J. J., Fernandez-Berridi, M. J., Roman, J. S. Polymer 1998, 39, 6891.
8. Ahn, S. J., Lee, K. H., Kim, B. K., Jeong, H. M. J Appl Polm Sci 2000, 78, 1861.
9. Zhang, L. L., Goh, S. H., Lee, S. Y., Hee, G. R. Polymer 2000, 41, 1429.
10. Lo, W. H., Yu, J. J Appl Polym Sci 2002, 83, 1036.
11. Choi, N. S., Kim, C. H., Cho, K. Y., Park, J.-K. J Appl Polym Sci 2002, 86, 1892.
12. Kim, C. H., Cho, K. Y., Choi, E. J., Park, J. K. J Appl Polym Sci 2000, 77, 226.
13. Avella, M., Errico, M. E. J Appl Polym Sci. 2000, 77, 232.
14. Chun, Y. S., Kim, W. N. J Appl Polym Sci 2000, 77, 673.
15. Willett, J. L., Kotnis, M. A., O'Brien, G. S., Fanta, G. F., Gordon, S. H. J Appl Polym Sci 1998, 70, 1121.
16. Organ, S. J., Barham, P. J. Polymer 1993, 34, 2169.
17. Varghese, H., Bhagawan, S. S., Someswara Rao, S., Thomas, S. Eur Polym J 1995, 31, 957.
18. Bucknall, C. B. Toughened Plastics; Applied Science Publishers: London, 1977.
19. Hoffman, J. D., Weeks, J. J. J Res Natl Bur Stand 1962, 66, 13.